Int. J. Mol. Sci. **2015**, *16*, 8505-8516; doi:10.3390/ijms16048505

OPEN ACCESS
International Journal of
Molecular Sciences
ISSN 1422-0067
www.mdpi.com/journal/ijms

Article

Decisive Interactions between the Heterocyclic Moiety and the Cluster Observed in Polyoxometalate-Surfactant Hybrid Crystals

Saki Otobe [1], Natsumi Fujioka [1], Takuro Hirano [1], Eri Ishikawa [2], Haruo Naruke [3], Katsuhiko Fujio [1] and Takeru Ito [1,*]

1 Department of Chemistry, School of Science, Tokai University, 4-1-1 Kitakaname, Hiratsuka 259-1292, Japan; E-Mails: sob0406@yahoo.co.jp (S.O.); sttok413@gmail.com (N.F.); tok413_st@yahoo.co.jp (T.H.); kfujio@tokai-u.jp (K.F.)

2 Department of Applied Chemistry, College of Engineering, Chubu University, 1200 Matsumoto, Kasugai, Aichi 487-8501, Japan; E-Mail: eishikawa@isc.chubu.ac.jp

3 Chemical Resources Laboratory, Tokyo Institute of Technology, 4259-R1-23, Nagatsuta, Midori-ku, Yokohama 226-8503, Japan; E-Mail: hnaruke@gmail.com

* Author to whom correspondence should be addressed; E-Mail: takeito@keyaki.cc.u-tokai.ac.jp; Tel.: +81-463-58-1211 (ext. 3737); Fax: +81-463-50-2094.

Academic Editor: Habil. Mihai V. Putz

Received: 22 December 2014 / Accepted: 1 April 2015 / Published: 16 April 2015

Abstract: Inorganic-organic hybrid crystals were successfully obtained as single crystals by using polyoxotungstate anion and cationic dodecylpyridazinium (C_{12}pda) and dodecylpyridinium (C_{12}py) surfactants. The decatungstate (W_{10}) anion was used as the inorganic component, and the crystal structures were compared. In the crystal comprising C_{12}pda (C_{12}pda-W_{10}), the heterocyclic moiety directly interacted with W_{10}, which contributed to a build-up of the crystal structure. On the other hand, the crystal consisting of C_{12}py (C_{12}py-W_{10}) had similar crystal packing and molecular arrangement to those in the W_{10} crystal hybridized with other pyridinium surfactants. These results indicate the significance of the heterocyclic moiety of the surfactant to construct hybrid crystals with polyoxometalate anions.

Keywords: inorganic-organic; polyoxometalate; surfactant; heterocyclic; hybrid crystal

1. Introduction

Weak chemical interactions, such as hydrogen bonding or van der Waals interactions, are crucial for the construction and function of biological molecules, such as proteins, DNA or RNA [1]. Employing these weak chemical interactions also provides effective options for building up synthetic molecular architectures [2–5]. To build up such molecular architectures, organic molecules or ligands are often used due to synthetic flexibility to control the directions and intensity of the weak chemical interactions. However, all-organic molecular architectures are less stable in the intermediate temperature (>100 °C) regions.

Inorganic-organic hybrid materials are more structurally stable than purely organic compounds owing to inorganic components, and the synergy of inorganic and organic characteristics will benefit constructing functional materials [6]. Conductive hybrid compounds composed of organic cations and inorganic anions have been reported, where the emergence of conductive functions is prompted by precise control of the molecular structures and arrangements of the components [7]. The precisely controlled inorganic-organic materials have been obtained as crystalline materials.

As a molecular inorganic component, polyoxometalates (POMs) are promising candidates with respect to their structural and functional controllability [8–16]. POMs with various physicochemical properties have been successfully hybridized by structure-directing surfactants [17–19] to construct inorganic-organic crystalline hybrids [20–24] and single crystals [25–34]. Among several POM-surfactant single crystals, utilizing surfactants with a heterocyclic moiety enables the precise control of the composition and structure [31–33]. However, the variation of the surfactants has been limited to pyridinium and imidazolium cations.

Here, we report the syntheses and structures of polyoxotungstate hybrid crystals containing heterocyclic surfactants, including the first example of a POM-surfactant crystal comprised of a pyridazinium surfactant. The decatungstate ($[W_{10}O_{32}]^{4-}$, W_{10}) anion was hybridized with dodecylpyridazinium ($[C_4H_4N_2(C_{12}H_{25})]^+$, C_{12}pda) and dodecylpyridinium ($[C_5H_5N(C_{12}H_{25})]^+$, C_{12}py) to form the crystals of C_{12}pda-W_{10} (**1**) and C_{12}py-W_{10} (**2**), respectively, and their chemical interactions and molecular arrangements were compared by X-ray structure analyses.

2. Results and Discussion

2.1. Crystal Structure of C_{12}pda-W_{10} (1)

C_{12}pda-W_{10} (**1**) was obtained by the cation exchange reaction of sodium salt of the W_{10} anion (Na-W_{10}). The retention of the W_{10} structure before and after the recrystallization was confirmed by infrared (IR) spectra, which exhibited the characteristic peaks in the range of 400–1000 cm^{-1} (Figure 1a–c). Suitable single crystals for X-ray crystallography were obtained by employing acetone as the crystallization solvent.

The X-ray structure and elemental analyses revealed the formula of **1** to be $[C_4H_4N_2(C_{12}H_{25})]_4[W_{10}O_{32}]\cdot 2(CH_3)_2CO$ (Table 1). Four C_{12}pda cations (1+ charge) were associated with one W_{10} anion (4− charge) due to the charge compensation. Figure 2 shows the crystal structure of **1**. The crystal packing consisted of alternating W_{10} inorganic monolayers and C_{12}pda organic bilayers with a periodicity of 24.5 Å (Figure 2a). The acetone molecules were placed at the interface between the W_{10} and C_{12}pda layers, being excluded from the inorganic layers. Although most C-C bonds of the dodecyl chains of C_{12}pda had the anti conformation, three C-C bonds (C8-C9, C41-C42, C54-C55) had the gauche conformation (Figure 2b), two of which (C8-C9, C41-C42) were located at some methylene groups far away from the hydrophilic head.

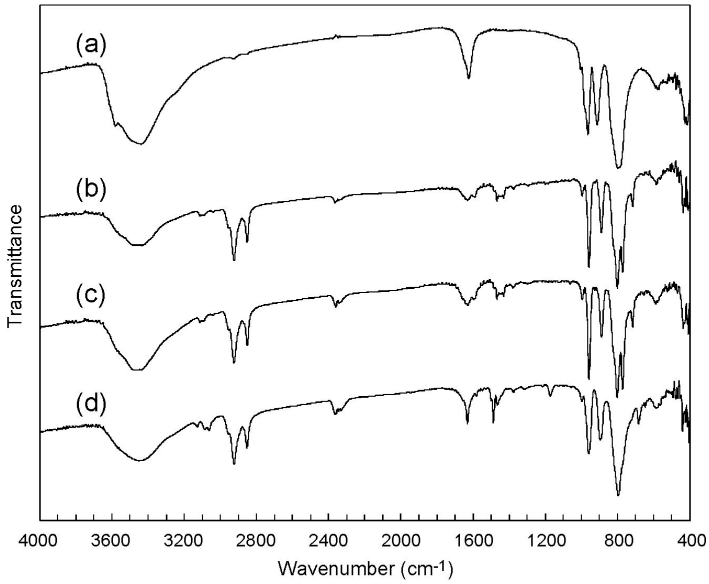

Figure 1. IR spectra of W_{10} compounds. (a) Na-W_{10} as a starting material; (b) As-prepared sample of **1**; (c) **1** after recrystallization; (d) As-prepared sample of **2**.

Table 1. Crystallographic data.

Compound	1	2
Chemical formula	$C_{70}H_{128}N_8W_{10}O_{34}$	$C_{76}H_{140}N_4W_{10}O_{36}$
Formula weight	3464.31	3524.45
Crystal system	triclinic	triclinic
Space group	$P\bar{1}$ (No.2)	$P\bar{1}$ (No.2)
a (Å)	10.55918(19)	10.813(7)
b (Å)	18.7700(3)	11.339(7)
c (Å)	25.4318(5)	23.610(13)
α (°)	74.4842(7)	99.415(9)
β (°)	86.5737(7)	91.558(5)
γ (°)	85.6363(7)	115.588(9)
V (Å^3)	4838.62(15)	2560(3)
Z	2	1
ρ_{calcd} (g·cm^{-3})	2.378	2.286
T (K)	193	173
μ (Mo·Kα) (mm^{-1})	11.924	11.272
No. of reflections measured	78,035	18,275
No. of independent reflections	22,146	11,774
R_{int}	0.0900	0.1384
No. of parameters	1106	563
R_1 ($I > 2\sigma(I)$)	0.0452	0.0983
wR_2 (all data)	0.1162	0.3237

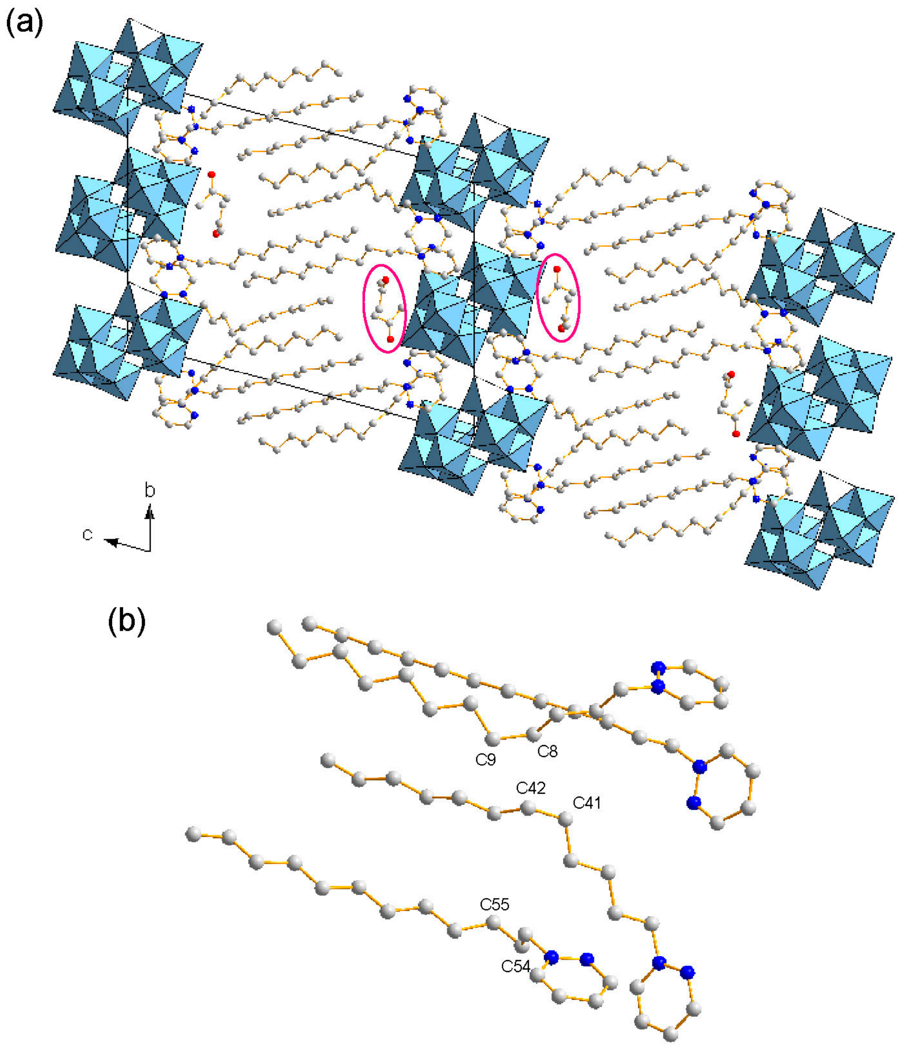

Figure 2. Crystal structure of **1** (C: gray, N: blue; W_{10} anions in polyhedral representations. H atoms are omitted for clarity). (**a**) Packing diagram along the *a* axis. Some acetone molecules are highlighted; (**b**) View of crystallographically-independent surfactant molecules.

The hydrophilic heads of C_{12}pda penetrated into the W_{10} inorganic layers and isolated each W_{10} anion (Figure 3a) in a similar way to that in the crystal of hexadecylpyridinium ($[C_5H_5N(C_{16}H_{33})]^+$, C_{16}py) and W_{10} (C_{16}py-W_{10}, **3**) [32]. However, the conformations of the heterocyclic moiety were different. In **1**, the pyridazine rings of the C_{12}pda cations were not in the vicinity of each other (Figure 3b), as in the case of the POM crystal comprising the pyridazinium cation without a long alkyl chain [35]. This indicates that there were no interactions, such as π–π stacking or the C-H···π interaction, between the heterocyclic moiety, being different from **2** (see below) and **3**. On the other hand, the pyridazine rings of C_{12}pda interacted rather more directly with the W_{10} anions. The crystals of **1** had several short contacts between of O atoms of W_{10} and C or N atoms of the pyridazine ring (2.88–3.22 Å (mean: 3.09 Å); Table 2), indicating the direct interactions between W_{10} and the heterocyclic moiety of C_{12}pda. The alignment of two crystallographically-independent W_{10} anions was not parallel, and the angle between the molecular C_4 axes was 8.3° (Figure 3b).

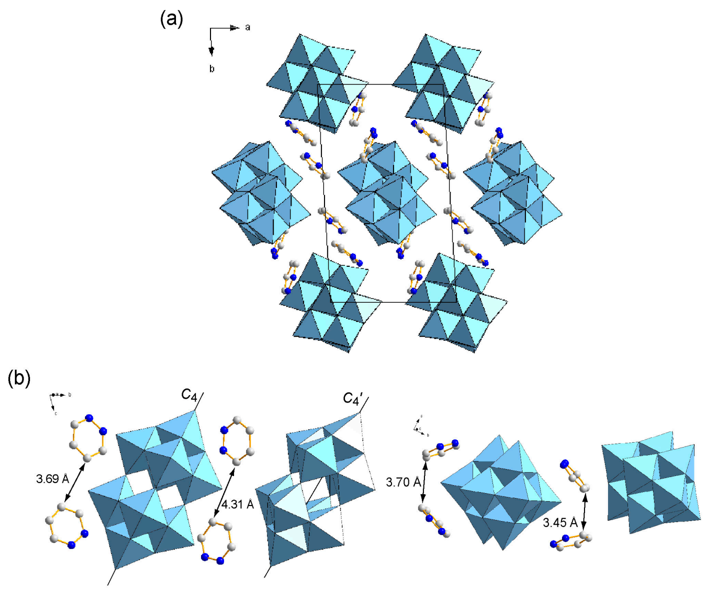

Figure 3. Molecular arrangements in the inorganic layers of **1** (C: gray, N: blue; W_{10} anions in polyhedral representations. H atoms and the dodecyl groups are omitted for clarity). (**a**) Packing diagram along the *c* axis; (**b**) View of crystallographically-independent pyridazinium moieties of surfactants in the vicinity of the W_{10} anions.

Table 2. Short contacts between W_{10} and the heterocyclic moiety of C_{12}pda in **1**.

Contact [a]	Distance (Å)	Contact [a]	Distance (Å)
$C20^{i}\cdots O1$	3.206	$C2\cdots O13$	3.118
$C20^{i}\cdots O2$	3.085	$C51^{iv}\cdots O13$	3.201
$C4\cdots O5$	3.210	$C33^{i}\cdots O20$	3.177
$C19^{i}\cdots O5$	3.147	$C49\cdots O22$	2.914
$C33^{ii}\cdots O6$	3.140	$C4\cdots O24$	2.886
$C34^{ii}\cdots O6$	3.180	$C17\cdots O25$	2.894
$C50^{iii}\cdots O7$	2.876	$C3^{ii}\cdots O27$	3.216
$C51^{iii}\cdots O7$	3.110	$C19^{ii}\cdots O27$	3.163
$C34^{iii}\cdots O8$	3.134	$C33^{i}\cdots O27$	3.142
$C4\cdots O9$	3.183	$C17^{i}\cdots O28$	3.135
$C3\cdots O9$	2.890	$C20\cdots O29$	3.119
$N8^{iii}\cdots O12$	3.046	$N6\cdots O30$	2.909

[a] Contact between O atoms of W_{10} and C or N atoms of the pyridazine ring of C_{12}pda. Symmetry codes: (i) $1 + x, y, z$; (ii) $-x, -y, 2 - z$; (iii) $1+x, -1 + y, z$; (iv) $x, -1 + y, z$.

In the crystal of **1**, The C_{12}pda cations had weak C-H···O hydrogen bonds [1]. Some C-H···O bonds were present in the vicinity of the gauche C-C bonds. The C···O distances were in the range of 2.89–3.74 Å (mean value: 3.32 Å), being much shorter than those of **2** (see below). In addition, most C-H···O hydrogen bonds were formed between W_{10} and the hydrophilic head of C_{12}pda, *i.e.*, the pyridazine ring of C_{12}pda. This suggests stronger interactions between W_{10} and the heterocyclic moiety of the surfactant in **1** than in **2**. These hydrogen bonds, as well as the electrostatic interaction between W_{10} and the heterocyclic moiety of C_{12}pda stabilized the layered crystal structure of C_{12}pda-W_{10} with rigid packing.

2.2. Crystal Structure of C_{12}py-W_{10} (2)

C_{12}py-W_{10} (**2**) was also synthesized by the cation exchange reaction of Na-W_{10} (Figure 1d). The molecular structure of W_{10} was retained before and after the recrystallization, as in the case of C_{16}py-W_{10} (**3**) [32]. Although the recrystallization of **2** was difficult, some crystals obtained from ethanol were able to be analyzed by X-ray crystallography.

The formula of **2** was revealed to be $[C_5H_5N(C_{12}H_{25})]_4[W_{10}O_{32}]\cdot 4C_2H_5OH$ (Table 1). Four C_{12}py cations (1+ charge) were associated with one W_{10} anion (4− charge), being similar to **1** and **3**. The crystal packing of **2** consisted of alternating W_{10} inorganic monolayers and C_{12}py organic bilayers with a distance of 23.2 Å (Figure 4a). Surprisingly, the cell parameters and the layered distances of **2** and **3** [32] were quite similar, even if the length of the pyridinium surfactants were changed to C_{12}py (**2**) from C_{16}py (**3**). The vacant spaces produced by changing to the shorter surfactant for **2** were filled by the ethanol molecules located at the interface between the W_{10} and C_{12}py layers. This similarity of the layered structures led to the similar molecular arrangements of W_{10} and the pyridine rings (see below). All C-C bonds in the dodecyl chains showed the anti conformation except one C-C bond (C7-C8) near the hydrophilic head of C_{12}py, being similar to that in **3** (Figure 4b).

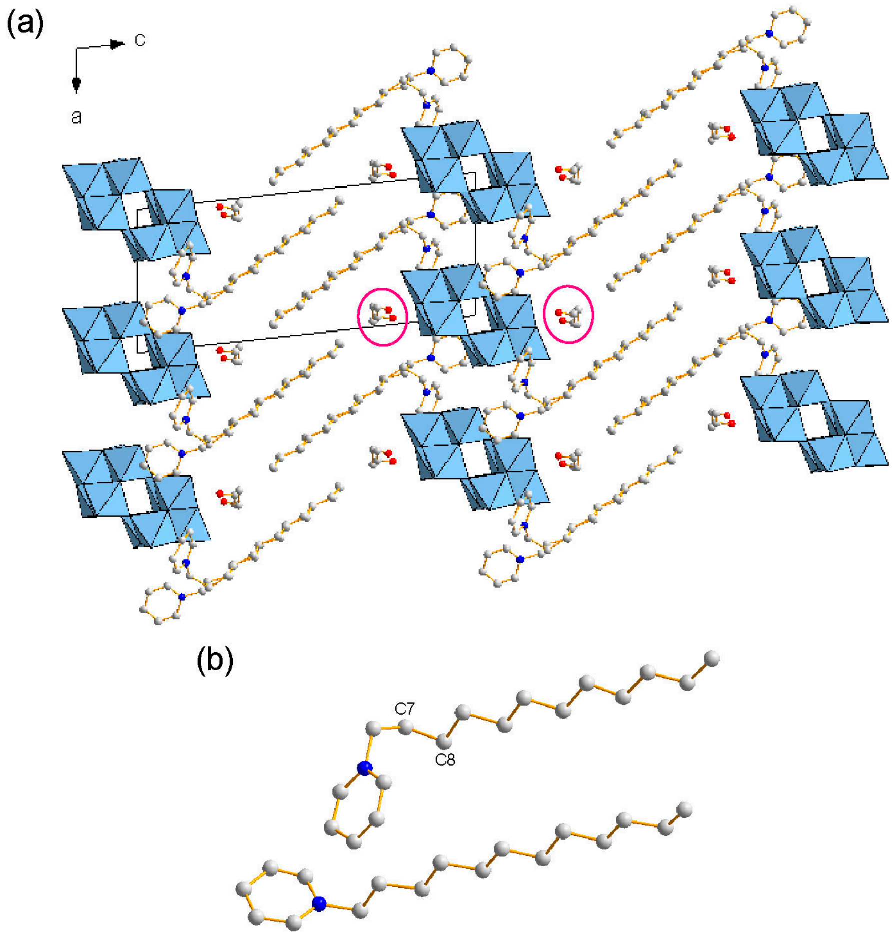

Figure 4. Crystal structure of **2** (C: gray, N: blue; W_{10} anions in polyhedral representations. H atoms are omitted for clarity). (**a**) Packing diagram along the *b* axis. Some ethanol molecules are highlighted; (**b**) View of crystallographically-independent surfactant molecules in **2**.

The hydrophilic heads of C_{12}py penetrated into the W_{10} inorganic layers in **2** (Figure 5a), which was almost the same manner as observed in **3**. The alignment of each W_{10} anion was parallel, being similar to **3**, but different from **1**. The penetrated C_{12}py cations formed two crystallographically-independent pairs (Figure 5b). The two C_{12}py cations interacted weakly through the C-H···π interaction, where the shortest interatomic distance was 2.91 Å for C3···H20 (Figure 5b). In the crystal of **2**, there were short contacts between W_{10} and the pyridine ring (2.93–3.22 Å (mean: 3.07 Å), Table 3). **2** also had C-H···O hydrogen bonds at the interface between the W_{10} and C_{12}py layers (C···O distance: 3.03–3.88 Å; mean value: 3.52 Å), being much longer than those observed in **1**. These longer C-H···O hydrogen bonds were formed around W_{10} and the pyridine ring of C_{12}py, indicating that the interactions between W_{10} and the heterocyclic moiety in **2** were weaker than in **1**. The structure of the heterocyclic moiety in the surfactants is the significant factor to construct the POM-surfactant hybrid crystals.

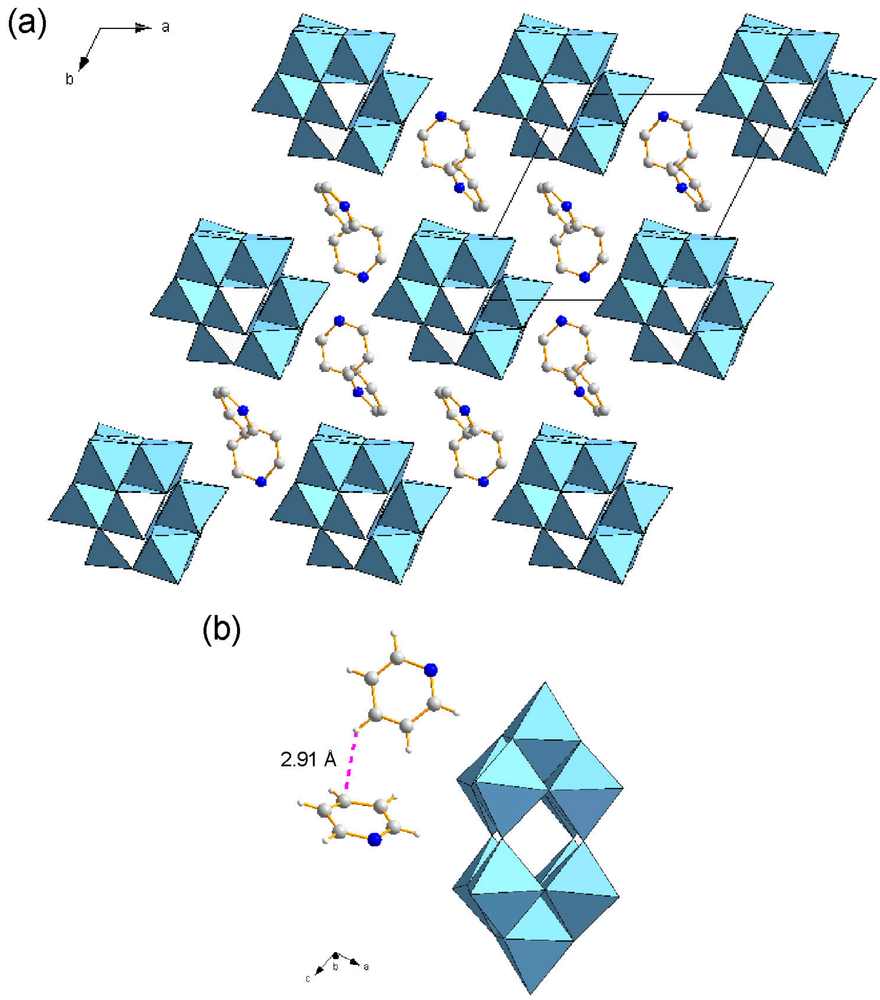

Figure 5. Molecular arrangements in the inorganic layers of **2** (C: gray, N: blue, H: white; W_{10} anions in polyhedral representations. The dodecyl groups are omitted for clarity). (**a**) Packing diagram along the *c* axis. H atoms are omitted for clarity; (**b**) View of crystallographically-independent pyridinium moieties of surfactants in the vicinity of the W_{10} anions. The selected short contact is presented as a pink dotted line.

Table 3. Short contacts between W_{10} and the heterocyclic moiety of C_{12}py in **2**.

Contact [a]	Distance (Å)	Contact [a]	Distance (Å)
C22···O5	3.153	C20^{ii}···O11	3.026
N2^{i}···O9	2.929	N1^{iii}···O14	2.960
C18^{i}···O9	2.980	C5^{iii}···O14	3.203
C22^{i}···O9	3.108	C21^{iv}···O14	3.091
C2···O11	3.220	C18^{v}···O16	3.031

[a] Contact between O atoms of W_{10} and C or N atoms of the pyridine ring of C_{12}py. Symmetry codes: (i) $-1 + x, y, z$; (ii) $1 - x, 1 - y, -z$; (iii) $x, -1 + y, z$; (iv) $1 - x, -y, -z$; (v) $-1 + x, -1 + y, z$.

3. Experimental Section

3.1. Syntheses and Methods

All chemical reagents were obtained from commercial sources (Wako, Osaka, Japan). $[C_4H_4N_2(C_{12}H_{25})]Br$ (C_{12}pda·Br) was synthesized by using pyridazine and 1-bromododecane based on the literature [36]. $Na_4[W_{10}O_{32}]$ (Na-W_{10}) was synthesized by combining a boiled solution of $Na_2WO_4 \cdot 2H_2O$ (0.5 M, 25 mL) and boiled HCl (1 M, 25 mL) [37].

C_{12}pda-W_{10} (**1**) was synthesized by the cation exchange of Na-W_{10}. Na-W_{10} (0.50 g, 0.20 mmol) was dissolved in 20 mL of HCl (pH = 2), and ethanol solution containing 0.27 g (0.81 mmol) of C_{12}pda·Br was added. After stirring for 10 min, the obtained white precipitates were filtered and dried. Recrystallization of the crude product from hot acetone gave colorless plates of **1**. The crystals of **1** were efflorescent, and its elemental composition was calculated for the formula without the solvent of crystallization. Data for **1**: anal. calcd. for $C_{64}H_{116}N_8W_{10}O_{32}$: C, 22.96; H, 3.49; N, 3.35%; found: C, 22.77; H, 3.36; N, 3.33%. IR (KBr disk): 996 (w), 958 (s), 889 (m), 800 (s), 772 (s), 589 (w), 437 (m), 407 (m) cm^{-1}.

C_{12}py-W_{10} (**2**) was synthesized by a similar procedure as for **1**. $[C_5H_5N(C_{12}H_{25})]Br$ (C_{12}py·Br, 0.28 g (0.81 mmol)) was employed as the cationic surfactant. The crude product was recrystallized from ethanol to obtain colorless prisms of **2**, which were efflorescent. Data for **1**: anal. calcd. for $C_{76}H_{120}N_4W_{10}O_{32}$: C, 24.42; H, 3.62; N, 1.68%; found: C, 24.01; H, 3.42; N, 1.62%. IR (KBr disk): 997 (w), 959 (s), 895 (m), 796 (s), 683 (m), 584 (w), 440 (m), 410 (m) cm^{-1}.

3.2. X-ray Diffraction Measurements

Single-crystal X-ray diffraction measurements for **1** were made on a Rigaku RAXIS RAPID imaging plate diffractometer with graphite monochromated Mo-Kα radiation (λ = 0.71075 Å). Diffraction data were collected and processed with PROCESS-AUTO [38]. The structure of **1** was solved by the charge flipping method [39] and expanded using Fourier techniques. The refinement procedure was performed by the full-matrix least-squares using SHELXL97 [40]. The measurements for **2** were made on a Rigaku Saturn70 diffractometer using graphite monochromated Mo-Kα radiation. Diffraction data were collected and processed with CrystalClear [41]. The structure of **2** was solved by direct methods [42] and expanded using Fourier techniques. The refinement procedure was performed by full-matrix least-squares using SHELXL2013 [42]. All calculations were performed using the CrystalStructure [43] software package. In the refinement procedure, all non-hydrogen atoms, except for C37 of **2**, were refined anisotropically, and the hydrogen atoms on C atoms were located in the calculated positions. The weak reflection intensities from the crystals of **2** may result in relatively high R_1 and wR_2 values. The results of checking cif files are available as supplementary materials. Further details of the crystal structure investigation may be obtained free of charge from the Cambridge Crystallographic Data Centre, 12 Union Road, Cambridge CB2 1EZ, UK; Fax: +44 1223 336 033; or E-Mail: deposit@ccdc.cam.ac.uk (CCDC 1055676-1055677).

4. Conclusions

Inorganic-organic hybrid crystals comprised of polyoxotungstate and surfactants having a heterocyclic moiety, $[C_4H_4N_2(C_{12}H_{25})]_4[W_{10}O_{32}]\cdot 2(CH_3)_2CO$ (**1**) and $[C_5H_5N(C_{12}H_{25})]_4[W_{10}O_{32}]\cdot 4C_2H_5OH$ (**2**), were successfully synthesized. Dodecylpyridazinium (C_{12}pda) and dodecylpyridinium (C_{12}py) were utilized as organic cations, and the decatungstate anion (W_{10}) was used for the inorganic component, which enabled the discussion of the effect of the heterocyclic moiety for the construction of the hybrid crystals. Although both hybrid crystals contained alternate stacking of W_{10} monolayers and interdigitated surfactant bilayers, pyridazine rings in **1** interacted more strongly with the W_{10} anions. **1** contained shorter C-H···O hydrogen bonds than those observed in **2**, indicating that these hydrogen bonds, as well as the electrostatic interaction between the C_{12}pda cation and the W_{10} anion stabilized the layered structure of C_{12}pda-W_{10} with rigid packing. On the other hand, **2** has similar cell parameters and molecular arrangements as those in the crystals of hexadecylpyridinium (C_{16}py) and W_{10} (**3**), also indicating the significance of the heterocyclic moiety for the construction of the hybrid crystals. The difference between the heterocyclic moieties led to different arrangements of W_{10} anions in **1** and **2**, which will contribute to the precise control of molecular arrangements and the emergence of characteristic conductivity.

Supplementary Materials

Supplementary materials can be found at http://www.mdpi.com/1422-0067/16/04/8505/s1.

Acknowledgments

This work was supported in part by the JSPS Grant-in-Aid for Scientific Research (No. 26410245) and the Research and Study Project of Tokai University Educational System General Research Organization.

Author Contributions

Saki Otobe and Takeru Ito conceived of and designed the experiments. Saki Otobe, Natsumi Fujioka and Takuro Hirano performed the experiments. Saki Otobe and Takeru Ito analyzed the data. Eri Ishikawa and Haruo Naruke contributed analysis tools. Katsuhiko Fujio contributed materials. Takeru Ito wrote the paper.

Conflicts of Interest

The authors declare no conflict of interest.

References

1. Desiraju, G.R.; Steiner, T. *The Weak Hydrogen Bond in Structural Chemistry and Biology*; Oxford University Press: New York, NY, USA, 1999.
2. Cockroft, S.L.; Hunter, C.A. Chemical double-mutant cycles: Dissecting non-covalent interactions. *Chem. Soc. Rev.* **2007**, *36*, 172–188.
3. Rebek, J., Jr. Simultaneous encapsulation: Molecules held at close range. *Angew. Chem. Int. Ed.* **2005**, *44*, 2068–2078.
4. Maurizot, V.; Yoshizawa, M.; Kawano, M.; Fujita, M. Control of molecular interactions by the hollow of coordination cages. *Dalton Trans.* **2006**, *2006*, 2750–2756.
5. Rosen, B.M.; Wilson, C.J.; Wilson, D.A.; Peterca, M.; Imam, M.R.; Percec, V. Dendron-mediated self-assembly, disassembly, and self-organization of complex systems. *Chem. Rev.* **2009**, *109*, 6275–6540.
6. Coronado, E.; Gómez-García, C.J. Polyoxometalate-based molecular materials. *Chem. Rev.* **1998**, *98*, 273–296.
7. Coronado, E.; Giménez-Saiz, C.; Gómez-García, C.J. Recent advances in polyoxometalate-containing molecular conductors. *Coord. Chem. Rev.* **2005**, *249*, 1776–1796.
8. Pope, M.T. *Heteropoly and Isopoly Oxometalates*; Springer: Berlin, Germany, 1983.
9. Hill, C.L. Polyoxometalates. *Chem. Rev.* **1998**, *98*, 1–390.
10. Long, D.-L.; Burkholder, E.; Cronin, L. Polyoxometalate clusters, nanostructures and materials: From self assembly to designer materials and devices. *Chem. Soc. Rev.* **2007**, *36*, 105–121.
11. Proust, A.; Matt, B.; Villanneau, R.; Guillemot, G.; Gouzerh, P.; Izzet, G. Functionalization and post-functionalization: a step towards polyoxometalate-based materials. *Chem. Soc. Rev.* **2012**, *41*, 7605–7622.
12. Okuhara, T.; Mizuno, N.; Misono, M. Catalytic chemistry of heteropoly compounds. *Adv. Catal.* **1996**, *41*, 113–252.
13. Sadakane, M.; Steckhan, E. Electrochemical properties of polyoxometalates as electrocatalysts. *Chem. Rev.* **1998**, *98*, 219–237.
14. Song, Y.-F.; Long, D.-L.; Ritchie, C.; Cronin, L. Nanoscale polyoxometalate-based inorganic/ organic hybrids. *Chem. Rec.* **2011**, *11*, 158–171.
15. Qi, W.; Wu, L. Polyoxometalate/polymer hybrid materials: fabrication and properties. *Polym. Int.* **2009**, *58*, 1217–1225.
16. Clemente-León, M.; Coronado, E.; Soriano-Portillo, A.; Mingotaud, C.; Dominguez-Vera, J.M. Langmuir–Blodgett films based on inorganic molecular complexes with magnetic or optical properties. *Adv. Colloid Interface Sci.* **2005**, *116*, 193–203.
17. Huo, Q.; Margolese, D.I.; Ciesla, U.; Demuth, D.G.; Feng, P.; Gier, T.E.; Sieger, P.; Firouzi, A.; Chmelka, B.F.; Schüth, F.; *et al.* Organization of organic molecules with inorganic molecular species into nanocomposite biphase arrays. *Chem. Mater.* **1994**, *6*, 1176–1191.
18. Kanatzidis, M.G. Beyond silica: Nonoxidic mesostructured materials. *Adv. Mater.* **2007**, *19*, 1165–1181.
19. Yamauchi, Y.; Kuroda, K. Rational design of mesoporous metals and related nanomaterials by a soft-template approach. *Chem. Asian J.* **2008**, *3*, 664–676.

20. Stein, A.; Fendorf, M.; Jarvie, T.P.; Mueller, K.T.; Benesi, A.J.; Mallouk, T.E. Salt-gel synthesis of porous transition-metal oxides. *Chem. Mater.* **1995**, *7*, 304–313.
21. Janauer, G.G.; Dobley, A.; Guo, J.; Zavalij, P.; Whittingham, M.S. Novel tungsten, molybdenum, and vanadium oxides containing surfactant ions. *Chem. Mater.* **1996**, *8*, 2096–2101.
22. Taguchi, A.; Abe, T.; Iwamoto, M. Non-silica-based mesostructured materials: hexagonally mesostructured array of surfactant micelles and 11-tungstophosphoric heteropoly anions. *Adv. Mater.* **1998**, *10*, 667–669.
23. Landsmann, S.; Lizandara-Pueyo, C.; Polarz, S. A new class of surfactants with multinuclear, inorganic head groups. *J. Am. Chem. Soc.* **2010**, *132*, 5315–5321.
24. Zhang, G.; Ke, H.; He, T.; Xiao, D.; Chen, Z.; Yang, W.; Yao, J. Synthesis and characterization of new layered polyoxometallates–1,10-decanediamine intercalative nanocomposites. *J. Mater. Res.* **2004**, *19*, 496–500.
25. Janauer, G.G.; Dobley, A.D.; Zavalij, P.Y.; Whittingham, M.S. Evidence for decavanadate clusters in the lamellar surfactant ion phase. *Chem. Mater.* **1997**, *9*, 647–649.
26. Spahr, M.E.; Nesper, R. Anhydrous octamolybdate with trimethyl hexadecyl ammonium cations. *Z. Anorg. Allg. Chem.* **2001**, *627*, 2133–2138.
27. Nyman, M.; Ingersoll, D.; Singh, S.; Bonhomme, F.; Alam, T.M.; Brinker, C.J.; Rodriguez, M.A. Comparative study of inorganic cluster-surfactant arrays. *Chem. Mater.* **2005**, *17*, 2885–2895.
28. Nyman, M.; Rodriguez, M.A.; Anderson, T.M.; Ingersoll, D. Two structures toward understanding evolution from surfactant-polyoxometalate lamellae to surfactant-encapsulated polyoxometalates. *Cryst. Growth Des.* **2009**, *9*, 3590–3597.
29. Yin, P.; Wu, P.; Xiao, Z.; Li, D.; Bitterlich, E.; Zhang, J.; Cheng, P.; Vezenov, D.V.; Liu, T.; Wei, Y. A double-tailed fluorescent surfactant with a hexavanadate cluster as the head group. *Angew. Chem. Int. Ed.* **2011**, *50*, 2521–2525.
30. Ito, T.; Sawada, K.; Yamase, T. Crystal structure of bis(dimethyldioctadecylammonium) hexamolybdate: a molecular model of Langmuir–Blodgett films. *Chem. Lett.* **2003**, *32*, 938–939.
31. Ito, T.; Mikurube, K.; Abe, Y.; Koroki, T.; Saito, M.; Iijima, J.; Naruke, H.; Ozeki, T. Hybrid inorganic-organic crystals composed of octamolybdate isomers and pyridinium surfactant. *Chem. Lett.* **2010**, *39*, 1323–1325.
32. Ito, T.; Fujimoto, N.; Uchida, S.; Iijima, J.; Naruke, H.; Mizuno, N. Polyoxotungstate-surfactant layered crystal toward conductive inorganic-organic hybrid. *Crystals* **2012**, *2*, 362–373.
33. Ito, T.; Ide, R.; Kosaka, K.; Hasegawa, S.; Mikurube, K.; Taira, M.; Naruke, H.; Koguchi, S. Polyoxomolybdate-surfactant layered crystals derived from long-tailed alkylamine and ionic-liquid. *Chem. Lett.* **2013**, *42*, 1400–1402.
34. Ito, T. Polyoxometalate-surfactant hybrids as building strategy for two-dimensional molecular arrays. *Polyoxometalate Chem.* **2012**, *1*, 6–14.
35. Ugalde, M.; Gutiérrez-Zorrilla, J.M.; Vitoria, P.; Luque, A.; Wéry, A.S.J.; Román, P. Synthesis, crystal structure, and thermal behavior of organically templated three-dimensional tunnel structures based on α-Keggin phosphododecamolybdate and diazines. *Chem. Mater.* **1997**, *9*, 2869–2875.
36. Fujio, K.; Ikeda, S. Size of spherical micelles of dodecylpyridinium bromide in aqueous NaBr solutions. *Langmuir* **1991**, *7*, 2899–2903.

37. Renneke, R.F.; Pasquali, M.; Hill. C.L. Polyoxometalate systems for the catalytic selective production of nonthermodynamic alkenes from alkanes nature of excited-state deactivation processes and control of subsequent thermal processes in polyoxometalate photoredox chemistry. *J. Am. Chem. Soc.* **1990**, *112*, 6585–6594.
38. Rigaku Corporation. *PROCESS-AUTO*; Rigaku Corporation: Tokyo, Japan, 2002.
39. Palatinus, L.; Chapuis, G. SUPERFLIP—A computer program for the solution of crystal structures by charge flipping in arbitrary dimensions. *J. Appl. Cryst.* **2007**, *40*, 786–790.
40. Sheldrick, G.M. SHELX97. A short history of SHELX. *Acta Cryst.* **2008**, *A64*, 112–122.
41. Rigaku Corporation. *CrystalClear*; Rigaku Corporation: Tokyo, Japan, 1999.
42. Sheldrick, G.M. SHELX2013. A short history of SHELX. *Acta Cryst.* **2008**, *A64*, 112–122.
43. Rigaku Corporation. *CrystalStructure 4.1*; Rigaku Corporation: Tokyo, Japan, 2014.